LA-UR -79-2834

TITLE: CALCULATION OF NEUTRON CROSS SECTIONS ON IRON BETWEEN 3 and 40 MeV

AUTHOR(S): E. D Arthur and P. G. Young

SUBMITTED TO: International Conference on Nuclear Cross Sections for Technology
Knoxville, Tennessee
October 22-26, 1979

los alamos
scientific laboratory
of the University of California
LOS ALAMOS, NEW MEXICO 87545

CALCULATION OF NEUTRON CROSS SECTIONS ON IRON BETWEEN 3 AND 40 MeV

E. D. Arthur and P. G. Young
Los Alamos Scientific Laboratory, University of California
Theoretical Division
Los Alamos, New Mexico 87545 U.S.A.

The use of high energy d+Li sources to produce neutrons for radiation damage studies will require evaluated neutron cross sections up to energies of 40 MeV. Experimental data in this energy region are scarce, and reliance must be placed upon nuclear model calculations to provide the necessary cross sections. We have thus calculated neutron-induced cross sections on ^{54}Fe and ^{56}Fe between 3 and 40 MeV using the multistep preequilibrium Hauser-Feshbach model code GNASH. Special care was taken in the determination of optical model parameters applicable over this wide energy range through use of, and comparison to, neutron total cross section and elastic angular distribution data, (p,n), and (α,n) data, as well as other high energy proton induced reaction cross sections and spectral results. The preequilibrium-statistical calculations using these parameters as well as gamma-ray strength functions, level densities, and discrete level information reproduce well most available experimental measurements above 3 MeV for varied reaction types including gamma-ray production data.

(^{54,56}Fe, Neutron Reactions, Evaluation, 3-40 MeV calculated σ(E,E',Ω), Hauser-Feshbach, Preequilibrium, DWBA Models)

To satisfy data needs of the Fusion Materials Irradiation Test Facility (FMIT), we have evaluated neutron induced cross sections on iron up to energies of 40 MeV. The results were then joined to the existing ENDF/B-V evaluation below 3 MeV

Since little experimental data, with the exception of total cross sections, exist for neutron energies above 20 MeV, the major portion of our evaluation relied upon results from nuclear model calculations. The reaction mechanisms governing neutron-induced reactions in this energy range can be described mainly by means of the Hauser-Feshbach statistical model along with corrections for preequilibrium and direct-reaction effects. For proper use of these models, suitable input parameters (optical model sets, gamma-ray strength functions, nuclear level densities, etc.) must be determined that are applicable over the entire energy range of interest in the calculation.

Neutron and charged particle transmission coefficients were calculated using spherical optical model parameters. For neutrons, these parameters should be constrained to provide reasonable agreement with higher energy experimental data while reproducing low energy information. By doing so, both the criteron of realistic compound-nucleus formation cross sections (important over the entire energy range) and reasonable behavior of low energy transmission coefficients [important in cases such as (n,2n) where low energy neutrons are emitted] can be met. We determined neutron optical parameters using the method developed by Lagrange[1] in which low energy resonance data are used simultaneously to supplement information obtained from fits to data at higher energies. The resulting parameters appear in Table I.

Proton and alpha particle optical parameters were determined using as a basis published sets obtained from experimental data fits in the mass and energy range of interest to our calculations. They were then adjusted to better reproduce data at low and high incident energies. For example, the Perey[2] proton optical potential was used with the addition of an energy dependent term in the imaginary potential to better fit reaction cross section data up to 50 MeV. The comparison of our calculated ^{55}Mn(p,n) cross section to experimental data (shown in Fig. 1) provides a measure of the low energy behavior of these parameters. A similar procedure was followed for the alpha-particle parameters we chose by making comparisons to ^{51}V(α,n) and ^{55}Mn(α,n) results.

TABLE I. Neutron Optical Parameters for Iron

	r(fm)	a(fm)
$V(MeV) = 49.747-0.4295E-0.0003E^2$	1.2865	0.561
$W_{SD}(MeV) = 6.053+0.074E$	1.3448	0.473
Above 6 MeV		
$W_{SD}(MeV) = 6.497-0.325(E-6.)$		
$W_{vol}(MeV) = -0.207+0.253E$	1.3448	0.473
$V_{SO}(MeV) = 6.2$	1.12	0.47

Gamma-ray competition to particle emission can be important, particularly around reaction thresholds. In our calculations, the average s-wave resonance parameters $\langle\Gamma_\gamma\rangle$ and <D> used to normalize gamma-ray transmission coefficients are not available or reliable for many of the compound systems involved. For this reason we have determined approximate gamma-ray strength functions assuming a giant dipole resonance shape from fits to ^{54}Fe and ^{56}Fe capture cross sections. Since such strength functions are expected to vary slowly over a limited mass region, we used similar forms for all compound nuclei.

Having determined consistent sets of input parameters, we then performed multistep Hauser-Feshbach calculations on ^{54}Fe and ^{56}Fe between 3 and 40 MeV using the GNASH[4] preequilibrium statistical model code. A sample decay chain used at higher energies is shown in Fig. 2. For each nucleus in the decay chain, we used the Gilbert-Cameron[5] level density model to describe the continuum excitation energy region along with available discrete level information. Preequilibrium corrections were made using the Kalbach[6] exciton model. Since the preequilibrium model could not adequately describe excitation by inelastic scattering of the collective ^{54,56}Fe levels, and since angular distribution information was needed, we performed DWBA calculations for 27 levels using deformation parameters determined from proton inelastic scattering.[7]

A sample of the calculated results for ^{56}Fe appear in Fig. 3 where major cross sections are shown from

their thresholds up to 40 MeV. At higher neutron energies, processes involving complex chains such as n,2np (sum of n,2np + n,npn + n,p2n) become important. For this reason, and in order to adequately describe gamma-ray production cross sections at higher energies, it was necessary to employ the complicated decay chain of Fig. 2 in which both neutron and proton decay paths were followed.

Recently measurements have been made of neutron and charged particle emission spectra at 15 MeV. Such data provide useful checks of the calculations, particularly with respect to preequilibrium corrections. Figure 4 compares our results to proton production spectra[8] measured for 15 MeV neutrons incident on ^{56}Fe, while Fig. 5 illustrates calculated and experimental[9,10] neutron emission spectra induced by 14.6 MeV neutrons.

In contrast to the lack of neutron differential data available above 20 MeV, there often exist proton reaction data, a comparison to which is useful in providing further checks upon the calculation of neutron induced cross sections at higher energies. We performed ^{56}Fe(p,xn) calculations using the parameters and techniques described above. The agreement between calculation and experiment shown in Fig. 6 lends confidence to our techniques and parameter values at higher incident energies.

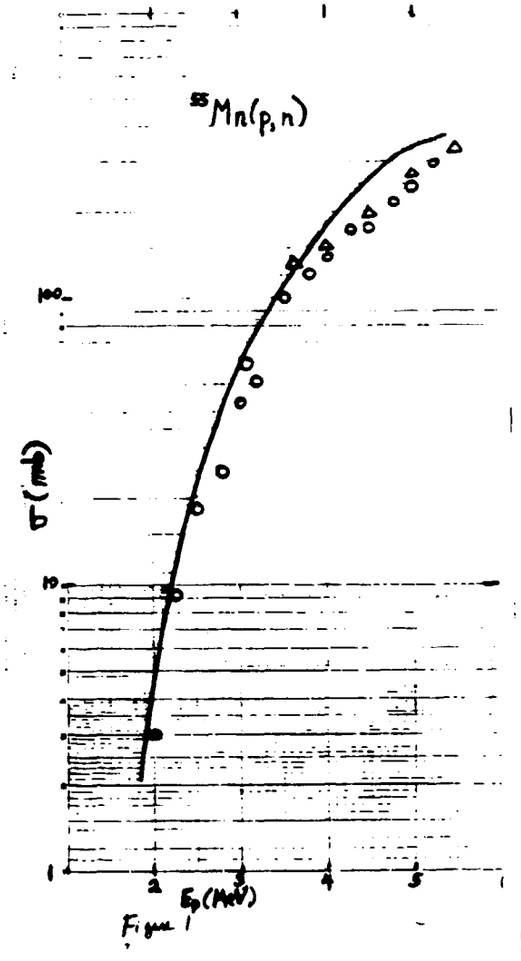

Fig. 1. Comparison of calculated and experimental data (Ref. 3) for ^{55}Mn(p,n).

REFERENCES

1. J. P. Delaroche, Ch. Lagrange, and J. Salvy, "Nuclear Theory in Neutron Nuclear Data Evaluation," IAEA-190 (1976).
2. F. G. Perey, Phys. Rev. 131, 745 (1962).
3. F. K. McGowan, "Nuclear Cross Sections for Charged-Particle Reactions," ORNL-CFX-1 (1966).
4. P. G. Young and E. D. Arthur, "GNASH - A Preequilibrium, Statistical Model Code for Calculation of Cross Sections and Spectra," LA-6947 (1977).
5. A. Gilbert and A. G. W. Cameron, Can. J. Phys. 43, 1446 (1965).
6. C. Kalbach, Z. Phys. A283, 401 (1977).
7. G. S. Mani, Nucl. Phys. A165, 225 (1977).
8. S. M. Grimes et al., Phys. Rev. C19, 2127 (1979).
9. D. Hermsdorf et al., "Differentielle Neutronenemissionsquerschnitte bei 14.6 MeV Einschussenergie," ZFK277 (1974).
10. G. Clayeux and J. Voignier, CEA-R-4279 (1972).
11. R. Michel et al., Nucl. Phys. A322, 40 (1979).
12. I. L. Jenkins and A. G. Wain, J. Inorg. Chem. 32, 1419 (1970).

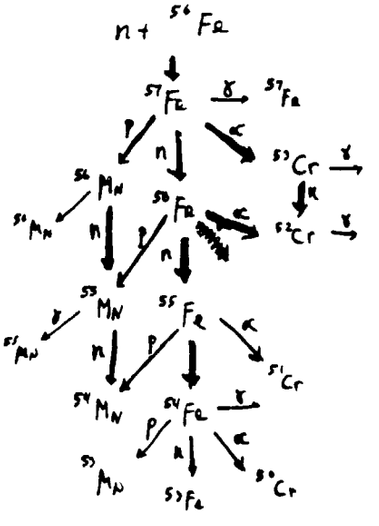

Fig. 2. Decay chain used for n + ^{56}Fe at higher energies.

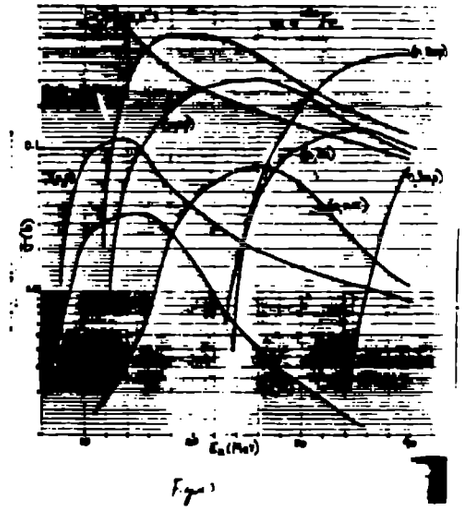

Calculated cross sections for $n + {}^{56}Fe$ up to 40 MeV.

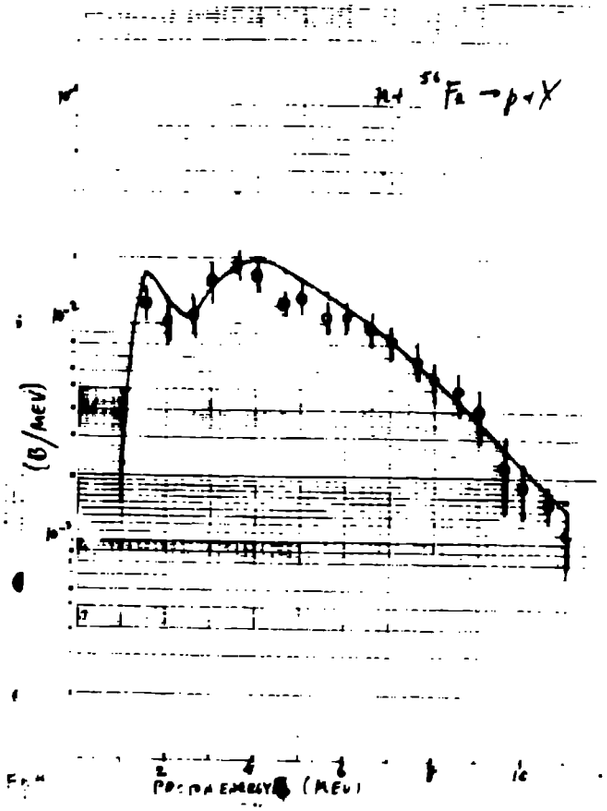

Experimental and calculated proton spectra for 15 MeV $n + {}^{56}Fe$

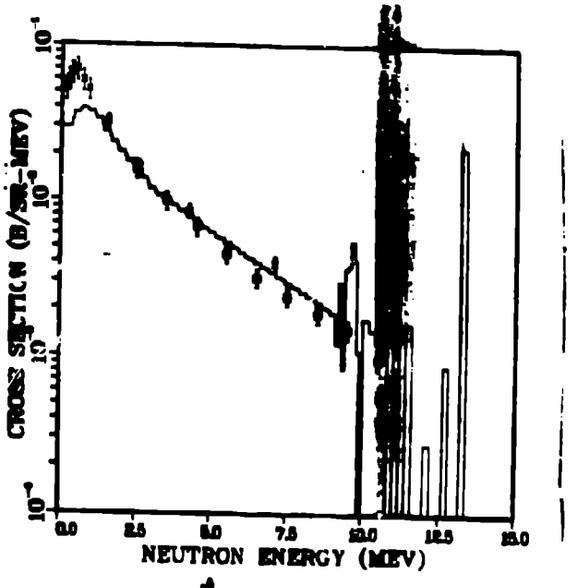

Comparison of the calculated and experimental neutron spectrum induced by 14.6 MeV neutrons on iron.

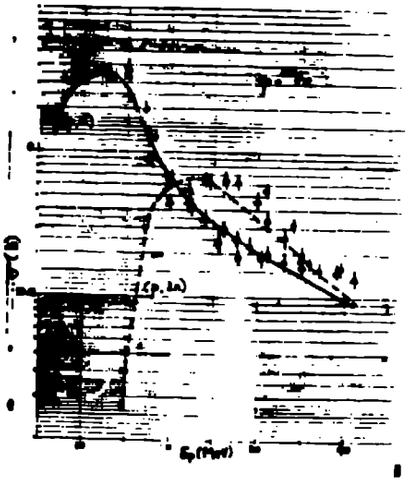

Ref. 8, 9

Calculated and experimental cross sections for the $^{56}Fe(p, xn)$ reactions.